CONF-841003--1

STUDIES OF A DIGITAL APPROACH TO NEUTRON DOSIMETRY AND MICRODOSIMETRY*

J. E. TURNER,[1] R. N. HAMM,[1] G. S. HURST,[1] H. A. WRIGHT,[1] M. M. CHILES,[2] and R. T. GREENE[3]

[1]Health and Safety Research Division
[2]Instrumentation and Controls Division
Oak Ridge National Laboratory
Oak Ridge, Tennessee 37831

and

[3]General Electric Company
Clearwater, Florida

CONF-841003--1

DE85 005371

Work has begun in an effort to develop a new, digital approach to neutron dosimetry. In contrast to analogue methods in current use, digital information describes the track of a recoil charged particle produced by a neutron in a gas in terms of the numbers of ions that occur in given volume elements of a detector. It appears that a device based on the time-projection chamber used in particle physics would enable one to measure relevant data for neutron dosimetry. Such an instrument would also furnish data sought in microdosimetry. In this paper we will describe the digital approach to dosimetry and will report on the initial Monte Carlo calculations of the detailed transport of protons and electrons in Ar, CH_4, and P-10 gases. These calculations are being used to assess the feasibility of constructing a practical chamber for use in neutron dosimetry and in microdosimetry.

1. THE DIGITAL APPROACH AND ITS OBJECTIVES

The objective of this work is to develop the theoretical and experimental foundations for a digital approach to neutron dosimetry and microdosimetry. Measurement of the numbers of electrons produced in various volume elements in a gas traversed by a charged recoil particle would provide a digital representation of that track. Conceptually, knowledge of the position and time coordinates of every electron produced would constitute "complete" information on the ionization events, from which quantities needed for neutron dosimetry and microdosimetry could be obtained. (Excitation of gas molecules also occurs, and is included in the calculations reported below.) Such detailed data would be expensive to obtain and would probably represent "overkill" in any dosimetric application. However, short of an ultimate instrument, a practical

*Research sponsored by the Office of Health and Environmental Research, U. S. Department of Energy, under contract DE-AC05-840R21400 with Martin Marietta Energy Systems, Inc.

device, based on the principle of time-projection chambers used in particle physics, appears to be feasible for obtaining a digital characterization of a charged-particle track. The purpose of this paper is to report on a specific concept being explored in a new, digital approach to neutron dosimetry and microsodimetry.

The new work consists of three distinct stages:

1. Development of a Monte Carlo computer code to calculate the transport and slowing down of neutron-recoil charged particles and all of their secondary electrons in a counter gas.
2. Using the Monte Carlo code to calculate responses for different potential chamber designs and to assess design parameters for a practical instrument.
3. Construction and testing of a device.

As described in this paper, we are presently at the beginning of the second stage. Results of calculations will be presented here for protons in one example of a possible chamber configuration.

2. MONTE CARLO COMPUTER CODE FOR CHARGED-PARTICLE TRANSPORT

As a chamber gas for study, we chose P-10, a mixture of 90% argon and 10% methane. The computer code has been written initially for the transport of electrons and protons, with carbon ions to be added as a next step. In principle, to carry out the transport calculations, one needs the microscopic differential cross sections for ionization, excitation, and elastic scattering in Ar and CH_4 for all relevant particles as functions of energy down into the thermal range. In addition, the cross sections for the inelastic events must be doubly differential (secondary-electron energy and angle). The necessary experimental data are lacking, particularly for the heavy ions at energies of several keV and below. Our code includes experimental data, where available, supplemented by a number of assumptions, as now described.

Proton Transport

We assume that a proton travels in a straight line as it slows down in the gas. At energies of several tens of keV and below, capture and loss of electrons by the proton considerably augments and complicates the production of ions. In effect, the capture and loss of a single electron by a proton produces an ion pair with only the expenditure of the energy with which the electron was originally bound. The additional process of ionization by neutral-atom collision, e.g., $H + Ar \rightarrow H + Ar^+ + e$, also occurs, with cross sections as large as those for ionization by the proton. While some experimental data are available for these processes in Ar, we have found little information for CH_4. In place of modeling the detailed processes connected with capture and loss, we have constructed phenomenological cross sections for ionization and excitation by protons in Ar and CH_4 that lead to the accepted stopping powers and W values at all energies. The argon cross sections are shown in Fig. 1. The ionization cross sections at 5 keV and above were obtained from the measurements tabulated by Rudd, Torburen, and Stolterfoht (1) and by Green and McNeal (2). We also used the secondary-electron energy spectra from Ref. (1), shown in Fig. 2, with the additional assumption that the spectrum at proton energies below 5 keV is the same as that at 5 keV.
The product of the excitation cross section and average energy loss by excitation were then selected to fit the stopping power. Assuming an average excitation loss of 11.3 eV leads to the excitation cross section

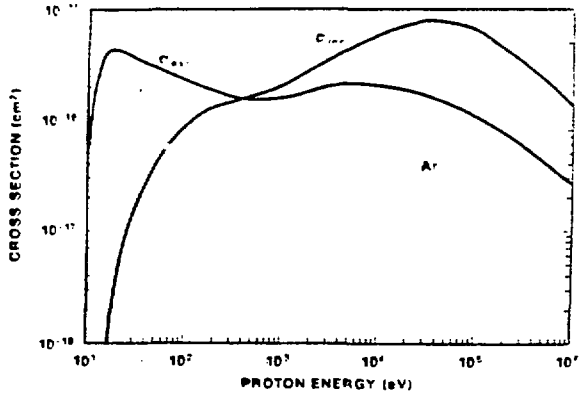

Fig. 1. Phenomenological ionization and excitation cross sections for protons in argon. These cross sections are consistent with stopping power and W values, but do not take explicit account of the capture and loss of electrons by protons or ionization produced by neutral hydrogen atoms.

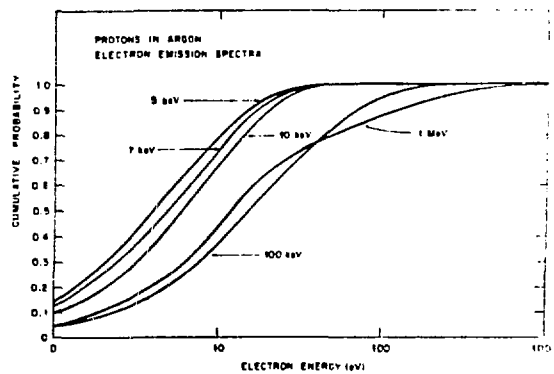

Fig. 2. Secondary-electron energy spectra for protons in argon from Ref. (1). The ordinate (cumulative probability) shows the probability that an ejected electron has an energy not exceeding the value given by the abscissa.

shown. The argon stopping power that we fit is shown in Fig. 3. The curve of Andersen and Ziegler (3) was used down to 1 keV, and we extrapolated it to lower energies as shown. The information on W values from ICRU Report 31 was used (4). No experimental data are reported for proton energies below 8 keV, and Report 31 recommends W = 27 ± 1 eV/ip for energies above 10 keV. In the calculations, W can be determined after the electron transport is included, as discussed next. Our calculated total numbers of electrons, N, produced by protons of different initial energies, E, stopping in argon and the corresponding W values are shown in Table 1. A similar set of data for cross sections, secondary-electron spectra, stopping power, and W values was compiled for CH_4, but will not be given here. The W value measurements for CH_4 made by Willems, Waibel, and Huber (5) for protons with energies down to 1 keV were used.

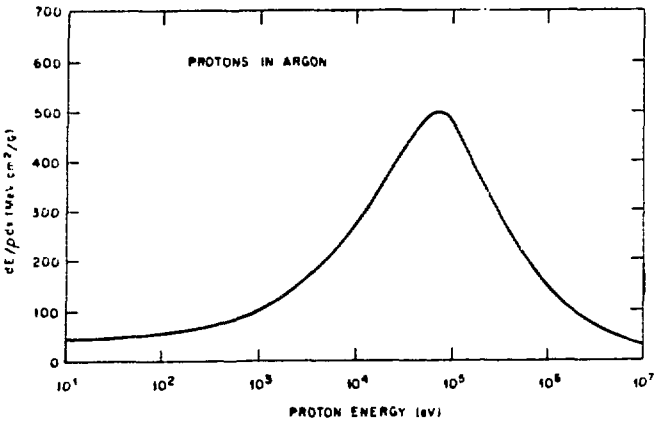

Fig. 3. Stopping power of argon for protons as a function of their energy.

Table 1

Average Number of Ion Pairs, N, and W Values for Protons of Energy, E, in Argon and Methane

	Argon		CH_4	
Energy E (keV)	N	W(eV/ip)	N	W(eV/ip)
0.5	10.9	45.7	13.6	36.8
1	26.4	37.8	30.1	33.3
2	59.6	33.6	63.2	31.7
5	164	30.5	162	30.8
10	342	29.3	327	30.6
20	698	28.7	657	30.4
50	1760	28.4	1650	30.4
100	3550	28.2	3300	30.3
250	8970	27.9	8240	30.3
500	18100	27.6	16500	30.3
1000	36600	27.3	33000	30.3

The following equations conveniently summarize the information that we have assembled for protons stopping in Ar and CH_4. The stopping power at any proton energy E is given by

$$-\frac{dE}{dx} = K\,(\sigma_{ion}\,\bar{Q}_{ion} + \sigma_{ex}\,\bar{Q}_{ex}), \qquad (1)$$

where K is the number of molecules per unit volume, σ_{ion} and σ_{ex} are the ionization and excitation cross sections (e.g., Fig. 1), and $\bar{Q}_{ion}$ and $\bar{Q}_{ex}$ are the average energies lost in ionization and in excitation collisions. (In the Monte Carlo calculations, individual energy losses are selected

from distributions in place of using $\overline{Q}_{ion}$ and $\overline{Q}_{ex}$.) The specific ionization (number of ions N per unit pathlength) of a proton is given by

$$\frac{dN}{dx} = K\,\sigma_{ion}\,(1 + \alpha), \tag{2}$$

where α is the average number of secondary electrons produced by an electron that is ejected directly by a proton. The differential W value, w, is then

$$w = -\left(\frac{dN}{dE}\right)^{-1} = \frac{-\,dE/dx}{K\,\sigma_{ion}\,(1 + \alpha)} \tag{3}$$

and the W value,

$$W = \frac{E}{\int_0^E -\left(\frac{dN}{dE}\right) dE} \tag{4}$$

Electron Transport

As seen from the measurements summarized in Fig. 2 for Ar, the spectrum of electrons ejected by proton collisions is generally very soft. At 10 keV, for example, virtually all electrons have energies less than 30 eV and ~80% have energies below the ionization potential, 15.8 eV, of argon. As a result, the quantity α in the above equations will be nearly zero at proton energies below 10 or 20 keV and the secondary-electron transport, therefore, will not be a critical factor at these lower proton energies. In view of this assessment, we have investigated some approximate ways of transporting electrons in place of assembling the complete cross-section data for Ar and CH_4, as was done for protons. The W values reported by Combecher (6) for electrons in the two gases down to very low energies are shown in Fig. 4. The sharp rise in W at energies below a few tens of eV reenforces the conclusion that α is near zero except for relatively high-energy protons. In one approximation, given an electron ejected with a certain energy by a proton collision, we used the curves in Fig. 4 to select an integral number of additional electrons that it would produce. The selection was made with an algorithm that gave the correct average implied by the curves. Proton W values close to those summarized in Table 1 were thus obtained. While this approximation led to satisfactory ionization yields, it did not provide a procedure for transporting the electrons. In a second approximation, we incorporated a modified version of an electron energy-loss and transport code that we developed for liquid water (7). The modifications of the existing code included "turning off" the collective effects that characterize the condensed phase. Other adjustments were also made until the W values were found to fall in the region of the two curves in Fig. 4. In the present version of our work, we calculate the electron transport by means of the modified water code, which appears to give a satisfactory representation of the secondary electrons for the purpose of studying chamber response. All electrons are followed in the calculations until they reach subexcitation energies, below the threshold for causing electronic transitions in the gas. Our final values of W and N, the average number of ion pairs produced, as functions of initial proton energy E are given in Table 1.

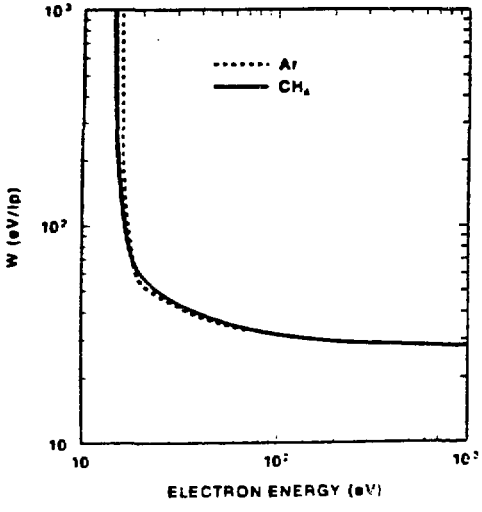

Fig. 4. W values for electrons in argon and methane as a function of the initial electron energy.

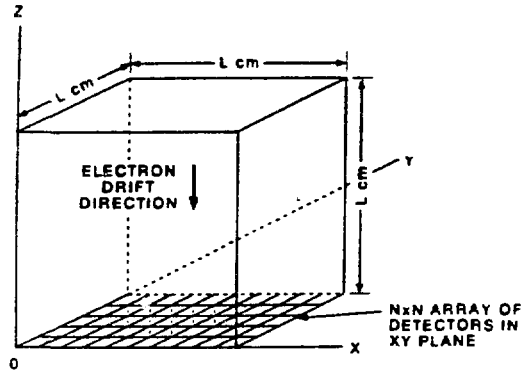

Fig. 5. Schematic configuration of time-projection chamber. Electrons from charged-particle track in chamber drift downward and trigger detectors to give their original (x,y) coordinates to within the grid resolution of $\pm$ L/N cm. Time of arrival gives the z coordinate.

3. TIME-PROJECTION CHAMBER

Fig. 5 shows schematically a configuration for a simple time-projection chamber (8), for which preliminary calculations are being made. The sensitive volume is a cube, having one corner at the origin of perpendicular XYZ axes as shown. The length of the edge of the cube is denoted by L (cm). Electrons produced by a charged particle in this volume drift toward the XY plane, in which an N x N array of equally spaced detectors, L/N cm apart in the X and Y directions, is located. The arrival of electrons in the XY plane triggers these detectors, giving to within $\pm$ L/N cm the (x,y) coordinates of ionizations produced by the charged particle, assuming that lateral electron diffusion is negligible. Diffusion is discussed in Ref. (8); it can be appreciable with low pressure and/or long drift distances. Diffusion can be neglected under the conditions considered here. The time of arrival in the XY plane provides the z coordinate. The parameters that are at one's disposal for the design of such a chamber are the chamber size L, the mesh size N of the detectors in the XY plane, the time resolution used to obtain the z coordinates, and the gas pressure. In practice, compromises in design will be dictated by factors of cost, feasibility, and practicality, as well as by the purpose for which such a device is to be used.

4. PRELIMINARY CALCULATIONS FOR A SAMPLE PROTON TRACK

We have carried out calculations for protons in a chamber with L = 10 cm and N = 10, thus having 1000 cubic sensitive-volume elements, each 1 cm^3 in size. Results will be presented here for a single proton track in the chamber in order to illustrate in detail a specific example of digital information. Figure 6 shows the calculated track of a 500-keV proton entering the chamber at the point x = 5.2 cm, y = 0.0 cm, and z = 8.7 cm, traveling parallel to the Y axis. Each dot in Fig. 6 represents

the position of one of the 168 subexcitation electrons that this particular proton produces in the chamber. The pressure is 1 torr. It is assumed in the calculations that these electrons are collected in the XY plane with neglibible lateral displacement.

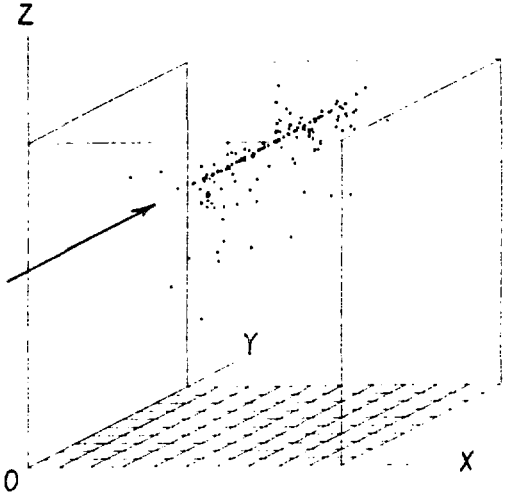

Fig. 6.
Distribution of subexcitation electrons (dots) in chamber after passage of a 500-keV proton, moving parallel to the Y axis and entering the chamber at x = 5.2 cm and z = 8.7 cm.

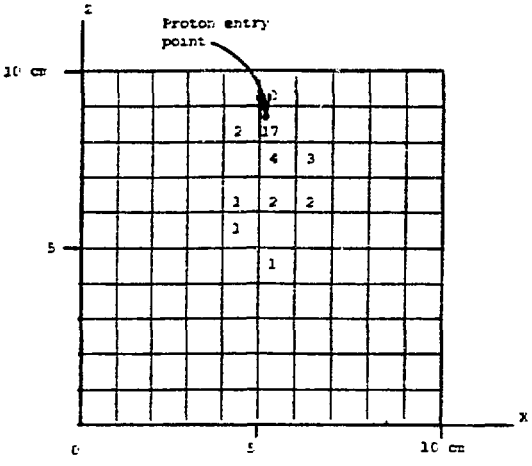

Fig. 7.
Numbers of subexcitation electrons in layer of cubes between y = 0 and y = 1 cm normal to incident proton, which entered slab at the point shown. No numbers are given in cells that contained no subexcitation electrons.

The numbers of subexcitation electrons that occur in the slab of cubes between y = 0 and y = 1 cm, normal to the proton's path, are shown in Fig. 7. There are 17 subexcitation electrons produced in the cube traversed by the proton, incident at the spot shown in the Figure. The numbers of electrons in the cubes behind this one, which are those also traversed by the proton, vary from 7 to 15. The energy deposited in each of these 10 cubes is found to be roughly proportional to the number of subexcitation electrons there. Energy-proportionality does not occur in cubes that contained smaller numbers of subexcitation electrons. The other nine slabs parallel to the XZ plane show some individual variations. Two slabs have electrons in only two cells.

When the subexcitation electrons produced by this proton and its secondaries drift vertically into the XY plane for collection, the total numbers reaching the detectors are given in Fig. 8. Their original positions above the plane are shown in Fig. 9. (The dots in the cell between x = 8 and x = 9 cm with two electrons are coincident, because identical positions are assigned when both electrons have subexcitation energies after an ionization.) As mentioned earlier, the arrival of the electrons in the XY plane can be resolved in time to infer the original z coordinates. The total energy deposited in the whole chamber is 4619 keV, and so one might infer a differential value w = 4619/168 = 27.49 eV/ip. However, the calculations show that 18 electrons escape from the chamber, carrying away 512 eV of kinetic energy. The proton actually loses 5100 eV and creates a total of 168 + 18 = 186 electrons. Assuming

that the escaping electrons produce a negligible number of additional ionizations, we obtain w = 5100/186 = 27.42 eV/ip for the differential value. This is in good agreement with the over-all integral value W = 27 ± 1 eV/ip recommended by the ICRU (4).

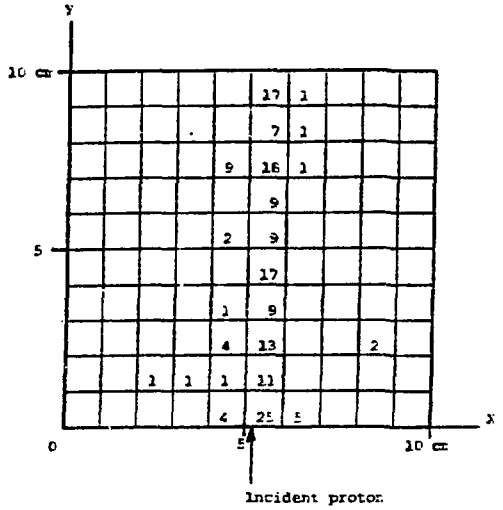

Fig. 8. Numbers of subexcitation electrons collected on the grid of detectors in the XY plane. The arrivals can be time-resolved to infer the original z coordinates of the electrons. No numbers are shown where no electrons appeared. Total number of electrons collected is 166.

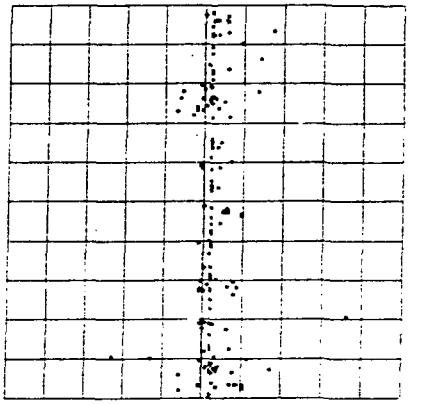

Fig. 9. View of track in Fig. 5 looking down on the XY plane. Dots show the positions of the subexcitation electrons within the individual boxes in Fig. 8.

The information contained in the signals from the detectors in the XY plane can be useful in a number of ways. Depending upon the application, different chamber designs would yield the digital characterization of the track in different ways. If, with high probability, there is no more than one electron in a given cell, then one can obtain a good assessment of that number. If there are $\gtrsim 5$ electrons in a cell, then one can also obtain a good assessment of that number. When the number of electrons is intermediate (e.g., 2, 3, 4), one is faced with significant fluctuations in the measurement process that makes assessment of the number of electrons uncertain.

There appears to be a "hierarchy" of designs for such a chamber, depending on the intended use. The most elaborate chamber, in principle, would resolve single electrons and provide complete spatial resolution of a track, as one would want for microdosimetric purposes. Each cell would be treated independently of all the others, and one would have the "most complete" information about a track. On a less elaborate scale, cells could be enlarged so that a large enough number of electrons occurred in most cells to enable the doses to be determined there. The distribution of this quantity, averaged over a large number of incident particles, would correspond to the single-event spectrum $f_1(z)$ in microdosimetry, where z is the specific energy. The integrated doses would give the distribution f(z;D) of the specific energy z at absorbed dose D. Also on this less elaborate scale, the total absorbed energy, combined

with the knowledge of the length of track, would provide the LET of the particle in the chamber gas. Finally, on a least elaborate scale, if one averages the total absorbed energy over the entire volume of the chamber, then one obtains the absorbed dose in the gas, as in conventional dosimetry.

The single proton track from Fig. 6 can be used to illustrate how distributions could be obtained for microdosimetry. For this single event, we plotted the frequency with which the 1-cm^3 cells in the chamber contain a given number of subexcitation electrons. The result is shown in Fig. 10. There are 832 cells with no electrons, 22 with one, 7 with 2

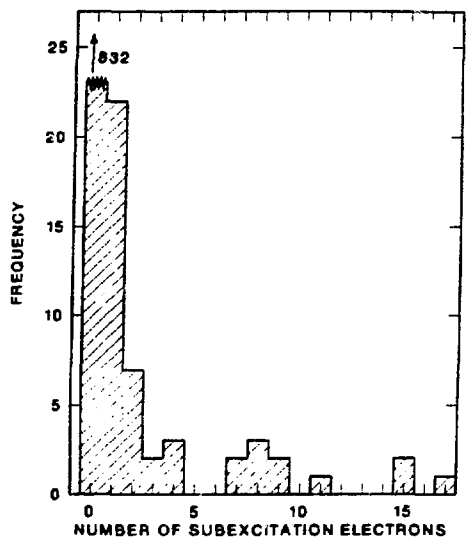

Fig. 10. Example of the frequency distribution of the number of subexcitation electrons produced in 1-cm^3 cubes after traversal of the chamber by a single 500-keV proton.

and so on, with a single cube containing a maximum of 17. The 10 cells which the proton crossed have the 10 highest numbers (7-17). One adjacent cell, not traversed directly by the proton, also contains 7 electrons. We stress that Fig. 10 was obtained by using only one proton and is not the average found by using a large number of protons. Alternatively, we could have plotted the specific energy, z, in each cell from this proton event. Either distribution is akin to the single-event spectrum in microdosimetry. The single-event spectrum could be obtained by making measurements for a large number of particles that irradiated the chamber under specified conditions. In place of the customary measurement of repeated events from single track segments in a detector, the event spectra would be obtained here by sampling over many segments of a number of tracks. In principle, very small volumes of unit-density material can be simulated by operating a large chamber at low pressure.

5. SUMMARY

The work reported here represents the first step in a digital approach to neutron dosimetry and microdosimetry. Further work will be aimed at adding carbon, argon, and possibly other recoil nuclei to the calculations and then looking toward the design of such a chamber. Construction of a prototype device is planned for laboratory testing.

REFERENCES

1. M. E. Rudd, L. H. Torburen, and N. Stolterfoht, At. Data and Nucl. Data Tables 23, 405 (1979).

2. A. E. S. Green and R. J. McNeal, J. Geophys. Res. 76, 133 (1971).

3. H. H. Anderson and J. F. Ziegler, Hydrogen, Stopping Powers and Ranges in all Elements, Pergamon Press, New York (1977).

4. ICRU Report 31, Average Energy Required to Produce an Ion Pair, International Commission on Radiation Units and Measurements, Washington, DC (1979).

5. G. Willems, E. Waibel, and R. Huber, Proceedings of the Eighth Symposium on Microdosimetry, p. 255, J. Booz and H. G. Ebert, Eds., Commission of the European Communities, Brussels, Belgium (1982).

6. D. Combecher, Rad. Res. 84, 198 (1980).

7. R. H. Ritchie, R. N. Hamm, J. E. Turner, and H. A. Wright, Proceedings of the Sixth Symposium on Microdosimetry, p. 345, J. Booz and H. G. Ebert, Eds., Commission of the European Communities, Brussels, Belgium (1978).

8. R. J. Maderas and P. J. Oddone, Time Projection Chambers, Physics Today 37(8), 36 (1984).

DISCLAIMER